





Imaging features of retroperitoneal extra-adrenal paragangliomas in 10 dogs

Alexis Gombert¹  | Alessia Diana²  | Silke Hecht³  | Stefano Nicoli⁴ |
 Federico Fracassi² | Jeremy Mortier⁵ | Edouard Reyes-Gomez^{6,7} | Pascaline Pey² 

¹ University Animal Hospital, Swedish University of Agricultural Sciences, Uppsala, Sweden

² Department of Veterinary Medical Science, Alma Mater Studiorum, University of Bologna, Ozzano Emilia, Italy

³ Department of Small Animal Clinical Sciences, University of Tennessee College of Veterinary Medicine, Knoxville, Tennessee, USA

⁴ Clinica Veterinaria Roma-Sud, Roma, Italy

⁵ Department of Small Animal Clinical Sciences, University of Liverpool, Neston, UK

⁶ Histology and Anatomical Pathology Unit, Ecole Nationale Vétérinaire d'Alfort, Maisons-Alfort, France

⁷ Ecole Nationale Vétérinaire d'Alfort, U955-IMRB, Inserm, UPEC, Maisons-Alfort, France

Correspondence

Alessia Diana, Department of Veterinary Medical Science, University of Bologna, Via Tolara di Sopra 50, I-40064 Ozzano Emilia, Bologna, Italy.
 Email: alessia.diana@unibo.it

[Correction added on 14 May 2022, after first online publication: CRUI funding statement has been added.]

Abstract

Retroperitoneal paragangliomas are rare tumors of the neuroendocrine system. Only a few canine case reports are available with rare descriptions of their imaging features. The objectives of this multi-center, retrospective case series study were to describe the diagnostic imaging features of confirmed retroperitoneal paragangliomas and specify their location. Medical records and imaging studies of 10 affected dogs with cytological or histopathologic results concordant with retroperitoneal paragangliomas were evaluated. Dogs had a median age of 9 years. Four of them had clinical signs and laboratory reports compatible with excessive production of catecholamines. Six ultrasound, four CT, four radiographic, and one MRI studies were included. The paragangliomas did not have a specific location along the aorta. They were of various sizes (median 33 mm, range: 9–85 mm of length). Masses had heterogeneous parenchyma in six of 10 dogs, regardless of the imaging modality. Strong contrast enhancement was found in all CT studies. Encircling of at least one vessel was detected in six of 10 masses, clear invasion of a vessel was identified in one of 10 masses. In five of 10 cases, the masses were initially misconstrued as lymph nodes by the on-site radiologist. Retroperitoneal paragangliomas appear along the abdominal aorta, often presenting heterogeneous parenchyma, possibly affecting the local vasculature, and displaying strong contrast enhancement on CT. Clinical signs can be secondary to mass effects or excessive catecholamine production. Underdiagnosis and misdiagnosis of this tumor are suspected as they can be silent, of small size, or confused with other structures.

KEYWORDS

canine, computed tomography, MRI, neuroendocrine, ultrasound

1 | INTRODUCTION

Paraganglia are derived from the neural crest and are associated with the autonomic nervous system.¹ They are nests of neuroendocrine cells disseminated all over the body and classified depending on their

anatomic location in respect to a specific nervous chain: parasympathetic and sympathetic.² Tumors arising from these structures are called paragangliomas and are classified similarly. Sympathetic paragangliomas are differentiated from analogous pheochromocytomas based upon their anatomic localization: only adrenal tumors can be called pheochromocytomas.³ Sympathetic paragangliomas typically secrete catecholamines in humans. The same is not considered to be true in dogs,⁴ although one case report identified catecholamine overproduction in a dog presenting with retroperitoneal paraganglioma.⁵ In

Abbreviations: AG, adrenal gland; STIR, short-tau-inversion-recovery; US, ultrasound.

Previous Presentation Disclosure: Abstract submitted to the 2021 EVDI online meeting.

EQUATOR Network Disclosure: An EQUATOR network checklist was not used in this study

This is an open access article under the terms of the [Creative Commons Attribution-NonCommercial](https://creativecommons.org/licenses/by-nc/4.0/) License, which permits use, distribution and reproduction in any medium, provided the original work is properly cited and is not used for commercial purposes.

© 2022 The Authors. *Veterinary Radiology & Ultrasound* published by Wiley Periodicals LLC on behalf of American College of Veterinary Radiology.

humans, the largest extra-adrenal accumulation of sympathetic paraganglionic tissue at birth is the organ of Zuckerkandl, caudal to the inferior mesenteric artery.⁶ Consequently, this is the typical site of sympathetic paragangliomas in people.^{2,7} Although few dogs display paragangliomas at the equivalent anatomic location, larger amount is situated ventrally to the aorta in the mid-retroperitoneum, most dogs also have small bodies next to the adrenal gland (AG).⁸ Because paragangliomas in dogs are usually biochemically silent, they are often detected incidentally.⁹ They may also cause a mass effect resulting in compromise of adjacent organs. Paragangliomas have been reported to cause ureteral obstruction in a cat,¹⁰ urinoma in a cougar,¹¹ and spinal cord compression in a dog.¹² If these neoplasms are functional, excess of catecholamines will create similar nonspecific, episodic clinical signs observed with pheochromocytomas.^{4,5}

Few retroperitoneal paragangliomas have been reported in dogs^{5,9,13-15} or have been included in studies evaluating pheochromocytomas¹⁶; all were identified adjacent to the anatomical location of the AG. Other studies have included diagnostic imaging description of parasympathetic paragangliomas affecting the head and neck,¹⁷⁻¹⁹ mediastinum,^{12,20,21} and spine²² of dogs. Aside from a single ultrasound and CT description in a dog¹⁵ or brief,⁵ nonspecific¹⁶ ultrasonographic characterization, no description of diagnostic imaging features of canine retroperitoneal paragangliomas are available to date. Apart from descriptions in human beings,²³⁻²⁶ this localization and type of neoplasm has only been described ultrasonographically in two cats^{10,27} and on CT study in a cougar.¹¹ In humans, CT examination is the preferred modality partly for its excellent spatial resolution.²⁸

The goal of this study was to describe the imaging features of confirmed retroperitoneal paragangliomas in a group of dogs and their topography relative to AGs and adjacent vessels.

2 | MATERIALS AND METHODS

2.1 | Experimental design and subject selection

Dogs with retroperitoneal paragangliomas were enrolled in this multicenter, retrospective, case series study. Databases of medical records from four university veterinary teaching hospitals and one private clinic were screened from 2008 to 2020 for canine patients that underwent abdominal imaging and had a confirmed diagnosis of retroperitoneal extra-adrenal paraganglioma. Imaging studies included CT, MRI, ultrasound (US), or a combination of them. The use of data was approved by each hospital. Institutional Animal Care and Use Committee approval was not needed for the review of the medical records. All decisions for subject inclusion or exclusion were made by a European College of Veterinary Diagnostic Imaging-certified veterinary radiologist (P.P. or J.M.) and a diagnostic imaging resident (A.G.).

Dogs were only included if they had at least one imaging study of the abdomen performed no more than 2 weeks before the diagnosis and if they had a cytological or histopathological diagnosis consistent with paraganglioma. Breed, age, sex, clinical reason for imaging study, and main clinical and laboratory findings were recorded by the diagnostic imaging resident (A.G.).

2.2 | Data recording

All imaging studies obtained were reviewed on an imaging software station (Osirix, Bernex, Switzerland) on a computer (MacBook Pro, macOS Catalina Version 10.15.7, Apple, One Apple Park Way, Cupertino, CA) by board-certified radiologists (European College of Veterinary Diagnostic Imaging, P.P. or J.M.) and a diagnostic imaging resident (A.G.). Initial imaging reports were recorded and reviewed a posteriori after blind assessment by the observers. Reports of abdominal radiographs or other included body parts in different modalities were also recorded. For CT studies, images before and after intravenous injection of iodinated contrast medium were used for evaluation, using a soft tissue algorithm and displayed with a soft tissue window (window width: 400 HU, window level: +40 HU). Multiplanar reformatted images were obtained for better characterization of the lesions. Cross-sectional images were evaluated for following criteria: size of tumor (maximal length, width, and height), shape (rounded, oval, irregular), margination (distinct, vague outline), enhancement pattern (homogeneous, heterogeneous), location and topography (using branches of the aorta and ipsilateral AG as landmarks), contact with adjacent organs, presence or absence of mass effect, number (uni- or bilateral, possible metastasis), as well as nature of other lesions if present. Specifically evaluated for CT images, pre- and postcontrast attenuation values were recorded: regions of interest were manually drawn over the masses while excluding mineralized and non-contrast enhancing areas, example is illustrated in Figure 1B. For MRI studies, all available sequences were evaluated. In these acquisitions, signal characteristics—compared to adjacent muscles—were evaluated.

Ultrasonographic images and video clips, when available, were reviewed. Ultrasonographic images were evaluated for the size of the tumor (length, width and height), shape (rounded, oval, irregular), margination (distinct, vague outline), echogenicity (compared to adjacent organs, homogeneous/heterogeneous), location and relative topography (using surrounding organs), contact with adjacent organs, presence or absence of mass effect, number (uni-, bilateral, possible metastasis), vascularization as assessed on Doppler examination (intensity, blood flow pattern), and nature of other lesions if present.

On each of these three modalities, the vascular relation with the tumor was assessed according to a grading system previously described.²⁹ The size of the AGs was collected for each dog, if possible, using the maximal caudal pole diameter and compared to previously suggested bodyweight-grouped cut-off values.³⁰ Diagnosis of paraganglioma was based on material obtained from US-guided fine-needle aspirates or biopsy, surgical resection, or necropsy. If performed, results of immunohistochemical profile for chromaffin cell markers were recorded. Corresponding reports, and surgery or necropsy reports, were documented.

2.3 | Data analyses

Descriptive analyses were performed by a diagnostic imaging resident (A.G.) Imaging features for each case were entered into a web-based application (Google sheets, Google LLC, Mountain View, California,

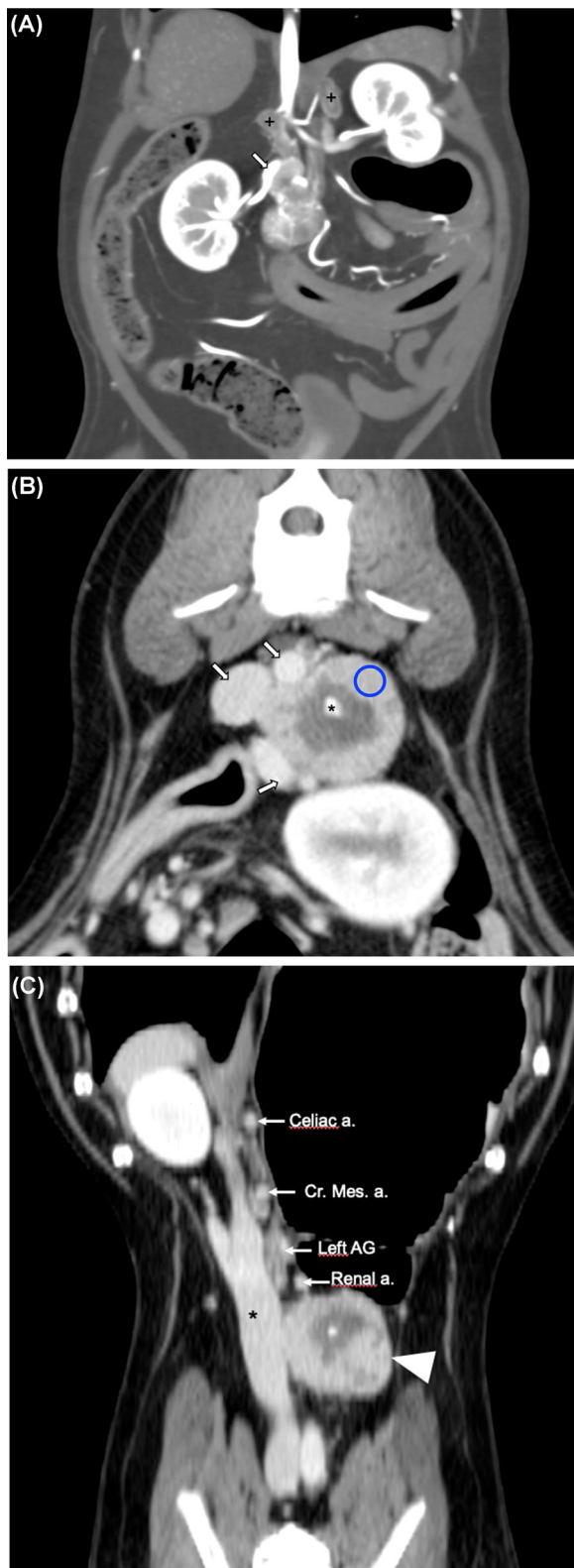


FIGURE 1 Computed tomography appearance of different retroperitoneal paragangliomas. Left is to the right. A, Case 4. Dorsal multiplanar reconstruction in minimal intensity projection in arterial phase after intravenous contrast injection in a 7-year-old neutered female Shih-Tzu displaying an oval mass with strong heterogeneous contrast-enhancement, multifocal mineralization foci, and close contact (grade-4) with the right renal vein (arrow), and ipsilateral adrenal gland (+). B, Case 6. Post-contrast CT images of a

USA). When cases included more than one diagnostic imaging modality assessment, cross-sectional imaging findings were given preference. Percentages and median values (range: minimum–maximum) were calculated.

3 | RESULTS

3.1 | Dogs

Ten dogs were included. Age ranged from 7 to 14 years with a median age of 9 years. Mixed breed accounted for four of the 10 dogs, Boxer breed for two, and one each of other breeds (German Shepherd dog, Shih Tzu, Australian Cattle dog, Jack Russel Terrier). There were four spayed females, three intact males, and three neutered males. The median bodyweight of the dogs was 15 kg (range: 5.5–38.5 kg). Individual signalment and clinical signs of the dogs is available in Supporting information 1.

3.2 | Clinical findings

On physical examination, four of 10 dogs presented an abdominal mass on palpation, one dog had a heart murmur, and six of 10 did not present any abnormalities. Reported reasons of the imaging study were nonspecific, they are summarized in Table 1. Among the three referred dogs, two had suspected adrenal nodules based on previous ultrasonographic assessment in the context of a splenic torsion or work-up of hypothyroidism, respectively. The third one was presented because of the growth of an already-diagnosed retroperitoneal paraganglioma despite varying doses of oral chemotherapy treatment (Toceranib phosphate, Palladia, Pfizer, Kalamazoo, Michigan).

3.3 | Laboratory findings

Various laboratory investigations were performed, including complete blood count and biochemistry in all dogs and urinalysis in five of 10 cases. In seven of 10 cases, results were within normal limits or

retroperitoneal paraganglioma in an 8-year-old German Shepherd Dog. Transverse plane in venous phase after intravenous contrast injection showing a rounded heterogeneous mass with mineralization focus (*) in close contact with three vessels (arrows): from dorsal to ventral, grade-2 with the aorta and caudal vena cava and grade-4 with the left renal vein. Example of ROI placement is demonstrated by the blue circle. C, Dorsal postcontrast multiplanar reformatted CT image illustrating the topography of the tumor (arrowhead) located caudally to the left renal artery (Renal a.). Note the caudal position and distance compared to the ipsilateral adrenal gland (Left AG) located caudally to the celiac (Celiac a.) and cranial mesenteric arteries (Cr. Mes. A.). The contact with the caudal vena cava (*) is visible. Images reconstructed with standard algorithm and displayed with a window width and window level of 40 HU and 400 HU. Images acquired in sternal recumbency, with a kVp of 120 (A,B,C), mA of 412 (A), 319 (B,C), and a slice thickness of 0.9 mm (A), 2.5 mm (B,C) [Color figure can be viewed at wileyonlinelibrary.com]

TABLE 1 Reported reason of imaging study

Clinical signs	
Dysorexia/anorexia	3/10
Lethargy	3/10
Hypertensive crises	3/10
Polyuria/polydipsia	2/10
Hematuria/dysuria	1/10
Polyphagia	1/10
Vomiting	1/10
Ataxia	1/10
Syncope	1/10
Physical examination finding	
Palpation of an abdominal mass	4/10
Other	
Suspected adrenal mass	2/10
Suspected retroperitoneal mass	1/10

unveiled minimal nonspecific abnormalities. Among these cases, specific endocrine tests were performed on two dogs: one had a normal response to adrenocorticotrophic hormone test stimulation and another had a normal urinary catecholamine to creatinine ratio. The remaining three dogs were also presenting hypertensive crises: all of them had an elevation of the secretion of catecholamines as assessed by the measurement of the concentration of metanephrines in plasma (2/3) or by a urinary normetanephrine to creatinine ratio (1/3). Two of these dogs were also tested for hyperadrenocorticism using low-dose dexamethasone stimulation or adrenocorticotrophic hormone test stimulation, one dog each, yielding results within normal limits.

3.4 | Diagnostic imaging findings

Four dogs underwent CT, one dog an MRI scan, six dogs had a US scan. One dog underwent US and CT with a 2-year time interval. The imaging technique details are available in Supporting Information 2.

The paragangliomas were left-sided (4/10) and right-sided (1/10), remaining cases were considered central when their localization was centered on the mid-line (5/10). Four AGs in three animals could not be identified on US exam (three right, one right AG); nonetheless, associated masses were conspicuously located caudally to the usual anatomic location of AGs. Compared with ipsilateral or closest AG, the masses were caudal in most cases (4/9), and if at the same level, medial (3/9) or lateral (2/9). Their localization was slightly more often centered between the origin of the phrenicoabdominal and renal arteries (3/10), followed by between the origin of the renal and ovarian or testicular arteries (2/10). Their localization is illustrated in Figure 2 and in the Supporting Information 3, also summarizing general diagnostic imaging findings. In one dog, available still US images did not allow to conclude on its position along the aorta. However, according to the medical record, it was found on the caudal third of the right ureter.

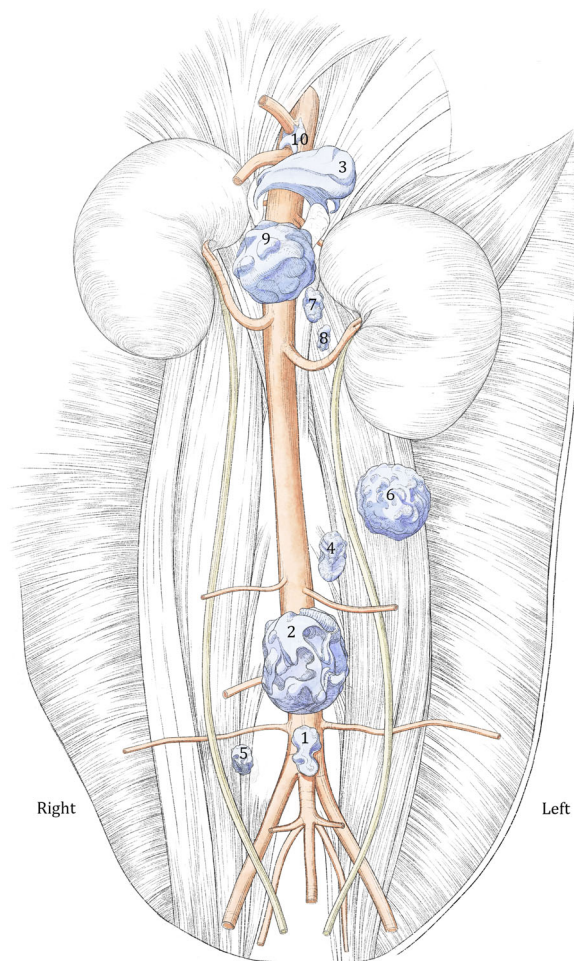


FIGURE 2 Representations of the different retroperitoneal masses of all included dogs. Each mass number matches the case number as shown in the Supporting Information 1 [Color figure can be viewed at wileyonlinelibrary.com]

Paragangliomas were defined as oval in most cases (6/10), round (1/10), and irregular (3/10) (bilobated, amorphous, or lobulated). Their margination was mainly distinct (9/10), and ill-defined in one case with capsular rupture (1/10). Margination of the mass assessed both on US and CT was first described as ill-defined on US but as distinct on the CT performed 2 years later. Mineralization was unfrequently identified (2/10). Paragangliomas had various sizes, with median length of 33 mm (range: 9–85 mm), median width of 23 mm (range: 4–80 mm), and median height of 18 mm (range: 4–72 mm). The mass reassessed in a 2-year period approximately gained 9 mm of length and 5 mm of height (38% increase; width not measurable on available US images). Effect of the masses on adjacent vasculature differed between cases. The caudal vena cava and the aorta were most commonly affected; grading on arterial vessels ranged from grade 1 to 5 whereas grading on venous vessels ranged from grade 1 to 7. In one case, clear invasion of the caudal vena cava was identified (grade-7), in other cases (4/10), this vessel and the renal and phrenicoabdominal veins were either totally compressed (grade-6), subject to a smoothly marginated mass effect (grade-4) or encircled (grade-3). The aorta was encircled in three of

10 cases, the celiac artery was subject to a mass effect with irregular margins in one case (grade-5). The third-largest mass compressed the cauda vena cava, created a smoothly marginated mass effect on the renal vein, and encircled the phrenicoabdominal vein, aorta, and the celiac, cranial mesenteric, and phrenicoabdominal arteries. The largest mass only had a small contact with the aorta (grade-2). In a 2-year span, one mass went from having a contact under-90° with two vessels (aorta and cranial mesenteric artery) to encircling four vessels (caudal vena cava, aorta, and ipsilateral renal artery and vein).

On CT, masses were heterogeneous in two of four cases with an attenuation of 30–50 HU (Figures 1 and 3). After intravenous injection of contrast medium, all masses presented a strong contrast enhancement in all phases. The four masses kept their pattern after injection of contrast medium. The perilesional fat attenuation was invariably normal. Computed tomography findings are compiled in Supporting Information 4.

Magnetic resonance imaging evaluation included T1-weighted (T1-W), T2-W, short-tau-inversion-recovery (STIR), and postcontrast T1-W with fat saturation sequences. When compared to adjacent muscles, the lesion was heterogeneous, hypointense on T1-W sequences, hyperintense on T2-W and STIR sequences, and displayed heterogeneous contrast enhancement on T1-W postcontrast images with fat saturation as shown on Figure 4. No gradient-recalled echo sequences were available.

Based on US images and video clips for two dogs masses were mostly heterogeneous (4/6), being cavitary in one case and including multiple small-sized round anechoic structures in another. Examples are displayed in Figures 5 and 6. The ultrasonographic features are summarized in Supporting Information 5. All paragangliomas were hypochoic compared to surrounding fat tissue, which appeared abnormally hyperechoic in one of six cases. Doppler interrogation was available in three cases, each evaluated as moderate amount of blood flow detected. In one, the radial pattern could be identified.

As assessed on CT, MRI, or US, contact with one or both AGs (3/10) or kidneys (2/10) was not uncommon with resulting mass effect in two and one cases, respectively, one AG being consequently deformed. Among the 17 AG included in the images, eight had dimensions considered enlarged with a median height of 6.9 mm (range: 5.0–9.9 mm).

According to diagnostic imaging reports, all dogs had unrelated other lesions. One dog also had a large hepatic mass and mottled spleen, later diagnosed as lymphoma; another had a urachal diverticulum abscess. Nodules were found in the spleen (3/10); left AG (1/10); testes (1/10), or in the subcutaneous tissues (1/10). Two dogs presented unilateral slight pyelectasia and associated perirenal fat stranding. Most of them displayed spinal degenerative changes. The retroperitoneal masses, later diagnosed as paragangliomas, were initially suspected to be of lymphoid nature in five of nine cases by involved radiologists. Four dogs had abdominal radiographs performed at the same time, where masses appeared as retroperitoneal soft-tissue opacity masses in three of four cases. The other one was of mixed-opacity, including multiple foci of mineralization. Thoracic radiographs were also performed in these four dogs and all CTs also included

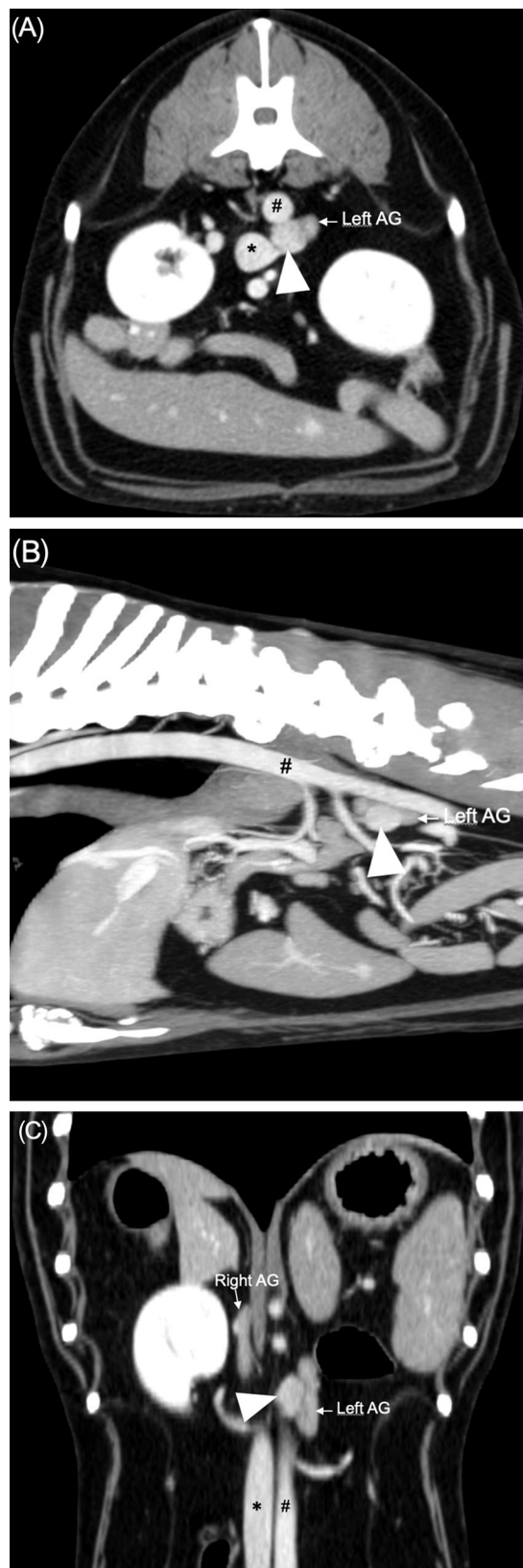


FIGURE 3 Postcontrast CT images of a retroperitoneal paraganglioma in case 7, a 13-year-old crossbreed neutered male dog. A, Transverse post-contrast CT image illustrating the tumor (arrowhead) demonstrating homogeneous contrast enhancement. Note the close contact with the caudal vena cava (*) and aorta (#) (both grade-2). B, Sagittal postcontrast multiplanar reformatted CT image

the thoracic part (4 dogs), yielding only incidental findings (spondylosis, mild cardiac silhouette enlargement, or subcutaneous bullet).

3.5 | Tissue sampling and analysis

Tissue samples were obtained via surgery (6/10), fine-needle aspiration (2/10), US-guided biopsy (1/10), or necropsy (1/10). In one case, aortic adhesion was surgically identified. Histology and immunohistochemistry were performed in five cases, histology alone in three cases, and cytology in two cases. The aforementioned deformed AG was normal on histological analysis after adrenalectomy. Only two dogs had a first diagnosis of paraganglioma; four samples were initially diagnosed as pheochromocytoma, and four others were suggestive of neuroendocrine neoplasia. Among the five immunohistochemical results, synaptophysin was positive in two cases, chromogranin was positive in two cases and negative in one, and cytokeratin was positive in one case and negative in two.

3.6 | Outcome

Outcome of four cases was available: one hypertensive dog underwent an excision of the paraganglioma and ipsilateral adrenalectomy, resulting in a complete normalization of its blood pressure. Another hypertensive dog received phenoxybenzamine treatment, without any effect on its blood pressure as assessed for 13 days. The follow-up was then lost for 7 months when the dog died due to foreign body ingestion. Concerning the dog followed for 2 years, after the first visit, it presented an excellent clinical condition except for the development of cutaneous flushing and pruritus not responding to antiparasitic treatments; secondary effect of the paraganglioma was suspected and antipruritic treatment was initiated. One dog, presenting with ataxia, was euthanized after CT acquisition for unrecorded reasons.

4 | DISCUSSION

This study described the diagnostic imaging features of retroperitoneal paragangliomas and their clinical presentation in 10 dogs. Interestingly, five of 10 cases were initially misconstrued as lymph nodes by on-site radiologists. Findings outlined converging characteristics among different diagnostic imaging modalities. Retroperitoneal paragangliomas were depicted as rather distinct oval to lobulated mass located along

illustrating topography of the tumor (arrowhead) located medially to the left adrenal gland (AG), ventrally to the aorta (#), caudally to the cranial mesenteric artery. C, Dorsal postcontrast CT image illustrating normal appearance of the left adrenal gland (Left AG) and medial position of the paraganglioma (arrowhead), ventrally to both aorta (#) and caudal vena cava (*). Images reconstructed with standard algorithm and displayed with a window width and window level of 40 HU and 400 HU. Images acquired in sternal recumbency, with a kVp of 120, mA of 319 and a slice thickness of 2 mm

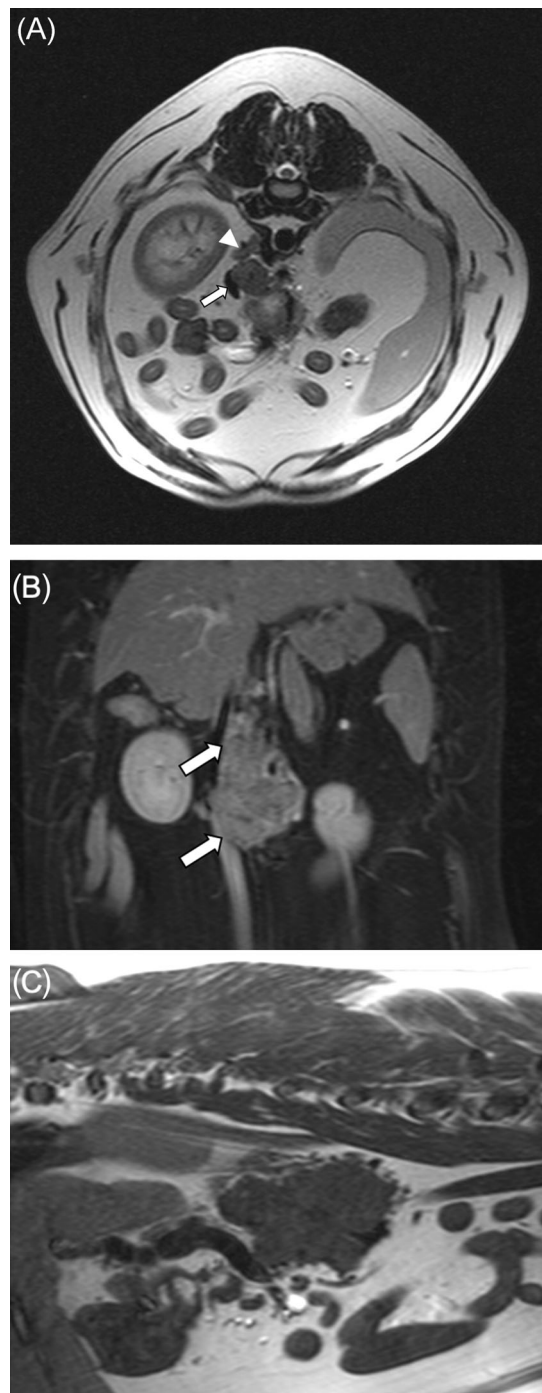


FIGURE 4 MRI acquisition (1.5 T) of the case 3, a 7-year-old neutered female Boxer dog. A, Transverse T2-weighted Spin-echo sequence, (TR: 5670 ms, TE 109 ms), 6-mm slice thickness. The mass is amorphous with ill-defined margination, heterogeneous and hyperintense compared to paraspinal muscles. It is here slightly right-sided. The caudal vena cava (arrow) is severely compressed. The right adrenal gland is dorsal (arrowhead) within normal limits. B, Dorsal T1-weighted with fat saturation sequence after intravenous contrast medium injection, (TR: 935 ms, TE: 14 ms) 6-mm slice thickness. The mass is heterogeneous and compresses the caudal vena cava (arrows): grade-6. C, Sagittal T1-weighted Spin-echo sequence, (TR: 246 ms, TE: 14 ms), 3-mm slice thickness: the mass is hypointense compared to paraspinal muscles and demonstrates irregular margins

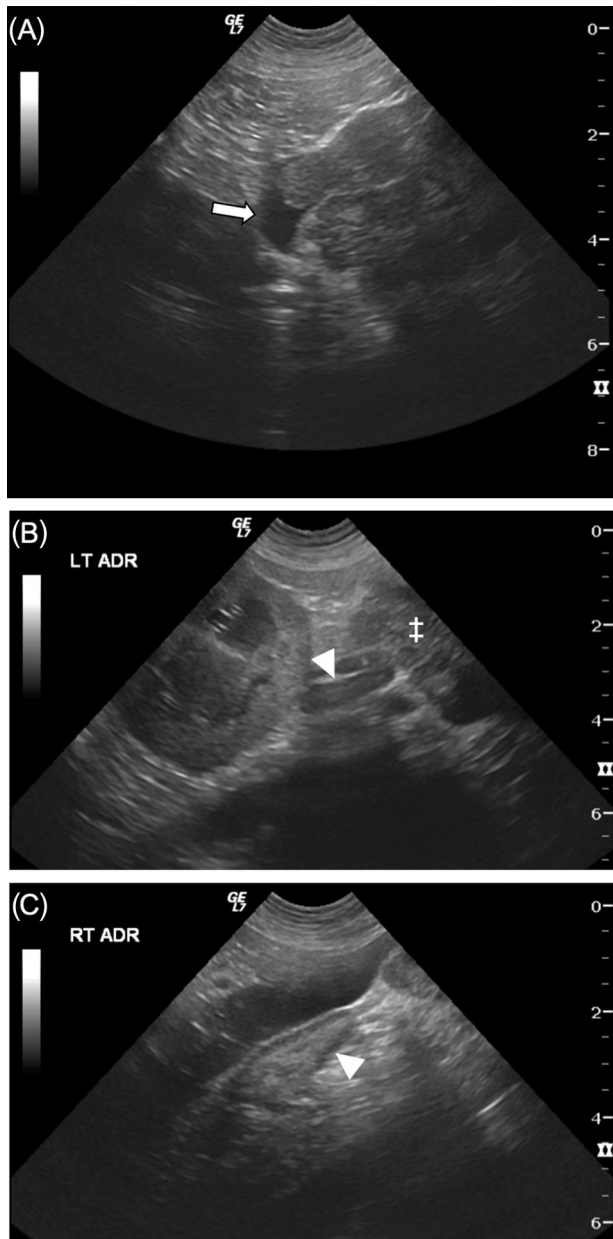


FIGURE 5 Ultrasonographic appearance of the mass of Case 9, (microconvex probe, 11 MHz) a 9-year-old neutered male Boxer dog: A, Lobulated hypoechoic mass with invasion of the caudal vena cava (arrow) is identified. B, The mass (‡) is in close proximity to the left adrenal gland (LT ADR, arrowhead), within normal limits. C, The contralateral adrenal gland (arrowhead) is within normal limits (RT ADR: right adrenal gland)

the aorta, as they are related to the sympathetic nervous system. They were mostly left-sided or central in the retroperitoneum, being often too large to be precisely assigned to one side. They were of various sizes, measuring under 1 cm in length in two cases and up to 7 cm diameter, in keeping with what is described in humans.^{23,31} Mineralization was uncommon, which is comparable to people where it is found in 10% of paragangliomas.^{23,26}

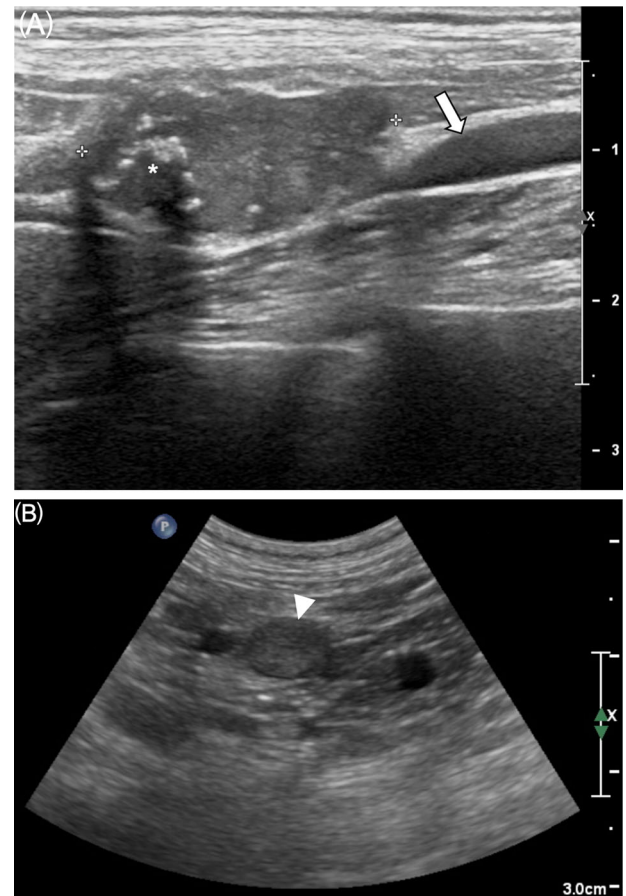


FIGURE 6 Ultrasonographic appearance of different retroperitoneal paragangliomas. A, Case 4, a 7-year-old neutered female Shih-Tzu (linear probe, 18 MHz). Oval heterogeneous nodule showing mineralization (*) and close contact with the caudal vena cava (arrow). B, Case 8. Microconvex probe, 8 MHz. Small rounded homogeneously hypoechoic nodule (arrowhead) representing a paraganglioma suspected to be hormonally active in 13-year-old crossbreed neutered male dog. The left renal artery is on the right of the image and left phrenicoabdominal artery on the left [Color figure can be viewed at wileyonlinelibrary.com]

Computed tomography features observed in our study were consistent with those described in pheochromocytoma in dogs where fast and strong contrast enhancement is common,^{32,33} and with the only previously described canine retroperitoneal paraganglioma.¹⁵ Rich capillary network and subsequent intense postcontrast attenuation are also described in humans^{23,25} and leopard.¹¹ Heterogeneity of the parenchyma is also a common finding in retroperitoneal paragangliomas in people as cystic changes, necrosis, hemorrhage, and mineralization are frequent.^{1,23,25}

The included MRI showed an amorphous heterogeneous mass. Paragangliomas often display a “salt-and-pepper” appearance in people, as flow voids from vascularity create punctate areas of low signal intensity and hemorrhage causes areas of hyperintense signal.^{1,23,26} Similarly, a case report of a paraganglioma in the cauda equina of a dog presented heterogeneous signal on T2-W images with well-defined

rounded hyperintense structures within the mass, likely representing cystic components.²²

In our case series, on US, most masses were heterogeneous with suggested rich vascular network. As stated previously, cystic and necrotic areas are common findings in paragangliomas in different species.^{26,33} Contrary to the findings of Pagani et al. concerning pheochromocytomas,³⁴ masses described in our study were often oval, well-delineated and nonencapsulated.

Consistent with the anatomic study describing the largest amount of paraganglial tissue between the AGs and the caudal mesenteric artery,⁸ we located most of the tumors cranial to the latter, with the most common location being bounded by the phrenicoabdominal and renal arteries. Quite similarly, previous case reports in dogs described masses positioned around the celiac artery,^{13–15} right AG,⁹ or caudal to the right kidney.⁵ In people, localization was found not to be associated with outcome.³⁵

Descriptions of pheochromocytoma in dogs have shown that they were likely to invade adjacent vessels.^{32,33} The different masses in this study had various effects on regional vessels. Interestingly, the largest mass was found to only be in mild contact with the aorta, whereas one of the smallest masses was compressing the ipsilateral phrenicoabdominal vein and in contact with the caudal vena cava and aorta. It is hypothesized that effects on vessels are conditional on anatomic location of the mass. Only one mass invaded the caudal vena cava. During surgery of one case, adhesion to the aorta was identified; this mass was described as encircling the vessel with distinct margins on CT. In total, encircling of at least one vessel was detected in six of 10 masses, highlighting the tendency of retroperitoneal paragangliomas to adhere to local vasculature.

In our study, older animals were affected (range 7–13 years), comparable to published case reports that included dogs aged 9 to 11 years.^{5,13–15} However, younger dogs may be affected as a mediastinal paraganglioma was described in a 1.5-year-old dog.¹² In humans, this neoplasia typically affects middle-aged adults without sparing pediatric patients.^{2,23,26}

Compared to US-extrapolated reference values for AG size, seven of 16 assessed AGs were enlarged. However, the difference was mostly minimal and could be secondary to variation of measurement and spatial resolution in each modality. Benign lesions of AGs are also common in older dogs, usually representing age-related hyperplasia.³⁴ Nonetheless, we cannot exclude a concomitant malignant process. In previously reported cases, one dog had concurrent nodular hyperplastic areas¹³ and another had a cortical adenoma.¹⁴ Four AGs were not identified during US examination; however, the location of each mass was considered too caudal.

In humans, most paragangliomas are functional, the excessive secretion of catecholamine causing paroxysmal or permanent hypertension.^{2,23} In our study, three dogs presented hypertensive crises, one also showing syncope. Abnormally elevated values of catecholamines were revealed. The cut-off of four times the upper normal limits, normally used to diagnose functional pheochromocytoma,³⁶ was not reached. However, the authors still strongly suspect functional paragangliomas as this cut-off is not sensitive in the diagnosis of

pheochromocytoma. Besides, one of these dogs showed symptom resolution after surgery. Another did not exhibit any known hypertensive crises, as this happens in 6.1% of pheochromocytomas and paragangliomas in people,³⁷ but presented recurring cutaneous flushing and pruritus not responding to antiparasitic treatments. A secondary effect of catecholamines was assumed as it has been described in functional pheochromocytoma.³⁸

Most of the usual symptoms associated with pheochromocytoma are nonspecific,³⁸ such as those presented by dogs of this study: lethargy, anorexia, vomiting, polyuria/polydipsia, or dysuria. In people, 30% of retroperitoneal paragangliomas and pheochromocytomas are estimated to be incidental findings.³⁷ In our study, three of 10 cases were incidentalomas. Silent cases are more likely to be larger in humans^{23,31} and therefore have space-occupying related consequences. Most masses were in contact with other organs such as kidneys and AGs, and some created mass effects on these organs but also on the intestinal tract, possibly creating identified nonspecific intestinal signs. Two dogs presented unilateral nephromegaly, pyelectasia, and retroperitoneal steatitis. It is therefore suspected that their masses created a partial ureteral obstruction. Such a consequence has been described before.^{10,11} Due to the paucity of published studies in veterinary medicine about retroperitoneal paragangliomas and as they can be very small, and located in a similar anatomic region, these masses were quite often (5/9) mistaken in imaging reports for enlarged renal or lumbo-aortic lymph nodes. In two cases, each with a mass localized around the renal artery, dogs were referred for an adrenal nodule, confusion supposedly due to their close locations.

In one study in people, the metastatic rate of retroperitoneal paraganglioma was 66%.³⁵ However, here, among the sampled lesions, no metastases were identified. Nevertheless, few of them presented uninvestigated nodules. In previously described canine cases of retroperitoneal paragangliomas, 2/4 had metastasis located in the mediastinum, liver, and heart.^{13,14} Similarly, splenic and hepatic metastases were found in leopard.¹¹ Nuclear imaging could identify metastases, as described in people.^{23,25} In two case reports of canine pheochromocytoma, the authors identified pheochromocytoma or metastasis using nuclear medicine.^{39,40}

The limits of this study are mainly related to its multicentric retrospective nature as imaging studies were performed with different machines, parameters, and protocols. Some clinical data were also partially missing. Cytologic and histopathologic diagnoses were variously denominated. As pheochromocytoma and paraganglioma are histologically and cytologically similar, lesions with a diagnosis of pheochromocytoma were considered paragangliomas because the sample did not involve an AG. Some samples had a nonspecific diagnosis of neuroendocrine tumors, but paragangliomas—or composite paragangliomas—were considered to be the only likely primary neuroendocrine tumor in the retroperitoneum. Metastatic tumors were excluded as no other neuroendocrine tumors were identified in included dogs. The small sample prevented any inferential statistical analysis.

To conclude, paragangliomas of the retroperitoneal space are rare neuroendocrine tumors located along the aorta, often presenting heterogeneous parenchyma, possibly affecting local vasculature and

displaying strong contrast enhancement on CT. These tumors are most likely underdiagnosed and misdiagnosed, as they can be silent, small-sized, or confused with enlarged lymph nodes or AGs. If they produce clinical signs, it can be secondary to direct catecholamine secretion and/or mass effect.

ACKNOWLEDGMENTS

Dr. Pascaline Pey is now working in the "Ospedale Veterinario I Portoni Rossi", Bologna, Italy and for Antech Imaging Services, Irvyne, California, USA. The author would like to thank Wladimir Peltzer for the illustrations.

Open Access Funding provided by Universita degli Studi di Bologna.

LIST OF AUTHOR CONTRIBUTIONS

Category 1

- (a) Conception and Design: Gombert, Diana, Pey
- (b) Acquisition of Data: Gombert, Diana, Hecht, Nicoli, Fracassi, Mortier, Reyes-Gomez, Pey
- (c) Analysis and Interpretation of Data: Gombert, Mortier, Pey

Category 2

- (a) Drafting the Article: Gombert, Pey
- (b) Revising Article for Intellectual Content: Gombert, Diana, Hecht, Nicoli, Fracassi, Mortier, Reyes-Gomez, Pey

Category 3

- (a) Final Approval of the Completed Article: Gombert, Diana, Hecht, Nicoli, Fracassi, Mortier, Reyes-Gomez, Pey

CONFLICT OF INTEREST

The authors have declared no conflict of interest.

ORCID

Alexis Gombert  <https://orcid.org/0000-0001-9387-6906>

Alessia Diana  <https://orcid.org/0000-0003-1709-3920>

Silke Hecht  <https://orcid.org/0000-0001-8805-836X>

Pascaline Pey  <https://orcid.org/0000-0003-3917-4756>

REFERENCES

1. Gill T, Adler K, Schrader A, et al. Extra-adrenal pheochromocytoma at the organ of Zuckerkandl: a case report and literature review. *Radiol Case Rep.* 2017; 12:343-347.
2. Moonim MT. Tumours of chromaffin cell origin: phaeochromocytoma and paraganglioma. *Diagn Histopathol.* 2012; 18:234-244.
3. Lam AK. Update on adrenal tumours in 2017 World Health Organization (WHO) of endocrine tumours. *Endocr Pathol.* 2017; 28: 213-227.
4. Galac S, Korpershoek E. Pheochromocytomas and paragangliomas in humans and dogs. *Vet Comp Oncol.* 2017; 15:1158-1170.
5. Robat C, Houseright R, Murphey J, et al. Paraganglioma, pituitary adenoma, and osteosarcoma in a dog. *Vet Clin Pathol.* 2016; 45:484-489.
6. Subramanian A, Maker VK. Organs of Zuckerkandl: their surgical significance and a review of a century of literature. *Am J Surg.* 2006; 192:224-234.
7. Chen H, Sippel RS, O'Dorisio MS, et al. The North American Neuroendocrine Tumor Society consensus guideline for the diagnosis and management of neuroendocrine tumors: pheochromocytoma, paraganglioma, and medullary thyroid cancer. *Pancreas.* 2010; 39:775-783.
8. Mascorro JA, Yates RD. The anatomical distribution and morphology of extraadrenal chromaffin tissue (abdominal paraganglia) in the dog. *Tissue Cell.* 1977; 9:447-460.
9. Dorn A, Theuring F, Dittert R, et al. A polypeptide immunoreactive nonchromaffin paraganglioma in the periglandular connective tissue of glandula suprarenalis of a dog. A case report. *Exp Pathol.* 1985; 27:99-104.
10. Borchert C, Berent A, Weisse C. Subcutaneous ureteral bypass for treatment of bilateral ureteral obstruction in a cat with retroperitoneal paraganglioma. *J Am Vet Med Assoc.* 2018; 253:1169-1176.
11. Duhamelle A, Langlois I, Pey P, et al. Malignant paraganglioma in a cougar (*puma concolor*). *J Zoo Wildl Med.* 2014; 45:994-998.
12. Rizzo SA, Newman SJ, Hecht S, et al. Malignant mediastinal extra-adrenal paraganglioma with spinal cord invasion in a dog. *J Vet Diagn Invest.* 2008; 20:372-375.
13. Ilha MRS, Styer EL. Extra-adrenal retroperitoneal paraganglioma in a dog. *J Vet Diagn Invest.* 2013; 25:803-806.
14. Rothacker TR, Pohlman L, Lin D, et al. Pathology in practice. *J Am Vet Med Assoc.* 2020; 256:1229-1232.
15. Couturier L, Guillaumot P, Duboy J, et al. Paraganglioma of a presumed celiac ganglion in a dog. *Vlaams Diergeneeskd Tijdschr.* 2014 Apr 30; 83(2):73-77.
16. Barthez PY, Marks SL, Woo J, et al. Pheochromocytoma in dogs: 61 Cases (1984-1995). *J Vet Intern Med.* 1997; 11:272-278.
17. Fischer M-C, Taeymans O, Monti P, et al. Orbital paraganglioma in a dog. *Tierärztl Prax Ausg K Kleintiere Heimtiere.* 2018; 46:410-415.
18. Mai W, Seiler GS, Lindl-bylicki BJ, et al. CT and MRI features of carotid body paragangliomas in 16 dogs. *Vet Radiol Ultrasound.* 2015; 56: 374-383.
19. Wisner ER, Nyland TG, Mattoon JS. Ultrasonographic examination of cervical masses in the dog and cat. *Vet Radiol Ultrasound.* 1994; 35: 310-318.
20. Sidor RE, Gambino J, Fraiser A, et al. What is your neurologic diagnosis?. *J Am Vet Med Assoc.* 2017; 250:1367-1371.
21. Yoon J, Feeney DA, Cronk DE, et al. Computed tomographic evaluation of canine and feline mediastinal masses in 14 patients. *Vet Radiol Ultrasound.* 2004; 45:542-546.
22. Duconseille A-C, Louvet A. Imaging diagnosis-paraganglioma of the cauda equina: mR findings. *Vet Radiol Ultrasound.* 2015; 56:E1-4.
23. Lee KY, Oh Y-W, Noh HJ, et al. Extraadrenal Paragangliomas of the Body: imaging Features. *Am J Roentgenol.* 2006; 187:492-504.
24. Ingram M, Barber B, Bano G, et al. Radiologic appearance of hereditary adrenal and extraadrenal paraganglioma. *Am J Roentgenol.* 2011; 197:W687-695.
25. Baez JC, Jagannathan JP, Krajewski K, et al. Pheochromocytoma and paraganglioma: imaging characteristics. *Cancer Imaging.* 2012; 12: 153-162.
26. Itani M, Mhlanga J. Imaging of Pheochromocytoma and Paraganglioma. In: Mariani-Costantini R, ed. *Paraganglioma: A Multidisciplinary Approach.* Codon Publications; 2019:41-61.
27. Friedlein RB, Carter AJ, Last RD, et al. The diagnosis of bilateral primary renal paragangliomas in a cat. *J S Afr Vet Assoc.* 2017; 88: 1412.
28. Neumann HPH, Young WF, Eng C. Pheochromocytoma and Paraganglioma. *N Engl J Med.* 2019; 381:552-565.
29. Pey P, Specchi S, Rossi F, et al. Prediction of vascular invasion and invasion of adjacent organs using a 7-point scale computed tomography grading system in adrenal tumors in dogs. *J Vet Intern Med.* Under review.
30. Soulsby SN, Holland M, Hudson JA, et al. Ultrasonographic evaluation of adrenal gland size compared to body weight in normal dogs. *Vet Radiol Ultrasound.* 2015; 56:317-326.

31. Wen J, Li H-Z, Ji G, et al. A decade of clinical experience with extra-adrenal paragangliomas of retroperitoneum: report of 67 cases and a literature review. *Urol Ann.* 2010; 2:12-16.
32. Gregori T, Mantis P, Benigni L, et al. Comparison of computed tomographic and pathologic findings in 17 dogs with primary adrenal neoplasia. *Vet Radiol Ultrasound.* 2015; 56:153-159.
33. Yoshida O, Kutara K, Seki M, et al. Preoperative differential diagnosis of canine adrenal tumors using triple-phase helical computed tomography. *Vet Surg.* 2016; 45:427-435.
34. Pagani E, Tursi M, Lorenzi C, et al. Ultrasonographic features of adrenal gland lesions in dogs can aid in diagnosis. *BMC Vet Res.* 2016; 12:267.
35. Ayala-Ramirez M, Feng L, Johnson MM, et al. Clinical risk factors for malignancy and overall survival in patients with pheochromocytomas and sympathetic paragangliomas: primary tumor size and primary tumor location as prognostic indicators. *J Clin Endocrinol Metab.* 2011; 96:717-725.
36. Quante S, Boretti FS, Kook PH, et al. Urinary catecholamine and metanephrine to creatinine ratios in dogs with hyperadrenocorticism or pheochromocytoma, and in healthy dogs. *J Vet Intern Med.* 2010; 24:1093-1097.
37. Kopetschke R, Slisko M, Kilisli A, et al. Frequent incidental discovery of phaeochromocytoma: data from a German cohort of 201 phaeochromocytoma. *Eur J Endocrinol.* 2009; 161:355-361.
38. Lunn KF & Page RL. Tumors of the Endocrine System. 2013;504-531.
39. Berry CR, Degrado TR, Nutter F, et al. Imaging of pheochromocytoma in 2 dogs using P-[18f] fluorobenzylguanidine. *Vet Radiol Ultrasound.* 2002; 43:183-186.
40. Head LL, Daniel GB. Scintigraphic diagnosis-an unusual presentation of metastatic pheochromocytoma in a dog. *Vet Radiol Ultrasound.* 2004; 45:574-576.

SUPPORTING INFORMATION

Additional supporting information may be found in the online version of the article at the publisher's website.

How to cite this article: Gombert A, Diana A, Hecht S, et al. Imaging features of retroperitoneal extra-adrenal paragangliomas in 10 dogs. *Vet Radiol Ultrasound.* 2022;63:393-402. <https://doi.org/10.1111/vru.13063>